Biosensors and Bioelectronics 152 (2020) 112007

Contents lists available at ScienceDirect

Biosensors and Bioelectronics

journal homepage: http://www.elsevier.com/locate/bios

A fully integrated bacterial pathogen detection system based on count-on-a-cartridge platform for rapid, ultrasensitive, highly accurate and culture-free assay

Won-Il Lee [a,1], Younghyeon Park [d,1], Sajal Shrivastava [b,1], Taekeon Jung [e], Montri Meeseepong [c], Jaelin Lee [d], Byeungwoo Jeon [d], Sung Yang [e], Nae-Eung Lee [a,b,c,*]

[a] Samsung Advanced Institute for Health Sciences & Technology (SAIHST), Sungkyunkwan University, 2066 Seobu-ro, Jangan-gu, Suwon, Gyeonggi-do, 16419, South Korea
[b] School of Advanced Materials Science & Engineering, Sungkyunkwan University, 2066 Seobu-ro, Jangan-gu, Suwon, Gyeonggi-do, 16419, South Korea
[c] SKKU Advanced Institute of Nanotechnology (SAINT), Sungkyunkwan University, 2066 Seobu-ro, Jangan-gu, Suwon, Gyeonggi-do, 16419, South Korea
[d] Department of Electrical and Computer Engineering, Sungkyunkwan University, 2066 Seobu-ro, Jangan-gu, Suwon, Gyeonggi-do, 16419, South Korea
[e] Department of Biomedical Science and Engineering, Gwangju Institute of Science and Technology (GIST), 123 Cheomdangwagi-ro, Gwangju, South Korea

ARTICLE INFO

Keywords:
Biosensor
Immunomagnetic concentration
Staphylococcus aureus
Food sample
Fluorescent imaging
Bacteria

ABSTRACT

Rapid, sensitive and accurate point-of-care-testing (POCT) of bacterial load from a variety of samples can help prevent human infections caused by pathogenic bacteria and mitigate their spreading. However, there is an unmet demand for a POCT device that can detect extremely low concentrations of bacteria in raw samples. Herein, we introduce the 'count-on-a-cartridge' (COC) platform for quantitation of the food-borne pathogenic bacteria *Staphylococcus aureus*. The system comprised of magnetic concentrator, sensing cartridge and fluorescent image reader with a built-in counting algorithm facilitated fluorescent microscopic bacterial enumeration in user-convenient manner with high sensitivity and accuracy within a couple of hours. The analytical performance of this assay is comparable to that of a standard plate count. The COC assay shows a sensitivity of 92.9% and specificity of 100% performed according to global microbiological criteria for *S. aureus* which is acceptable below 100 CFU/g in the food matrix. This culture-independent, rapid, ultrasensitive and highly accurate COC assay has great potential for places where prompt bacteria surveillance is in high demand.

1. Introduction

Bacterial pathogens are common causes of infectious diseases and food-borne illnesses. Every year, 550 million people fall ill from consuming pathogen-contaminated food (WorldHealthOrganization, 2019). Numerous infectious diseases caused by pathogenic bacteria account for yearly deaths of 5.2 million (Hessling et al., 2017). In some cases, consuming food-borne bacteria can lead to deadly diseases such as sepsis and hemolytic uremic syndrome (Vygen-Bonnet et al., 2017; Wachi et al., 2005). In order to prevent fatalities from pathogenic bacteria and stop their spread, it is necessary to develop a rapid, highly sensitive and accurate point-of-care testing (POCT) system that can detect bacterial concentrations as low as 10 colony forming unit/mL (10 CFU/mL) or less in food homogenates or body fluids within a couple of hours in resource-constrained or urgency-demanding environments (Reddy et al., 2018). However, the conventional culture-based bacterial count method for detection of food-borne pathogenic bacteria or pathogenic bacteria in body fluids is time-consuming, requiring 3–5 days (Goldmeyer et al., 2008; Puttaswamy et al., 2011; Wang and Salazar, 2016).

Specifically, in the food industry there is a time gap between the fresh food supply and inspection from samples, resulting in food poisoning by pathogenic bacteria from uninspected products. To fill this gap, researchers have developed a variety of methods with shortened time for detecting food-borne pathogenic bacteria with high sensitivity and specificity, such as nucleic acid-based (Chen et al., 2012; Nezhad,

* Corresponding author. Samsung Advanced Institute for Health Sciences & Technology (SAIHST), Sungkyunkwan University, 2066 Seobu-ro, Jangan-gu, Suwon, Gyeonggi-do, 16419, South Korea.
E-mail address: nelee@skku.edu (N.-E. Lee).
[1] These authors contributed equally to this work.

https://doi.org/10.1016/j.bios.2020.112007
Received 18 November 2019; Received in revised form 2 January 2020; Accepted 4 January 2020
Available online 7 January 2020
0956-5663/© 2020 Elsevier B.V. All rights reserved.

2014; Ryu et al., 2013; Zhou et al., 2013) and immunological-based methods (Chaivisuthangkura et al., 2013; Kim et al., 2019). Both of these methods have been successfully commercialized. However, the molecular detection kits and lateral flow assay (LFA) kits currently available still require culturing of target bacteria in liquid media as a pre-enrichment step. To avoid this time-consuming step, other bacteria separation and concentration methods such as centrifugation (Fukushima et al., 2007), filtration (Li et al., 2013; Wolffs et al., 2006) and magnetic-based separation (Uyttendaele et al., 2000) have been investigated. Unlike centrifugation and filtration, in which a series of concentration steps may decrease the recovery of bacteria (Wang and Salazar, 2016), magnetic separation and concentration has become a major approach due to its rapidness (Joshi et al., 2009), easy manipulation (Chen et al., 2014; Poshtiban et al., 2013) and good recovery (Yang et al., 2013), followed by development of magnetic separation and concentration integrated with well-commercialized technologies such as polymerase chain reaction (PCR) (Mao et al., 2016; Yang et al., 2013) and the LFA method (Li et al., 2017; Stewart et al., 2017). Although these detection methods combined with the magnetic separation and concentration technique significantly reduce total assay time, they are still limited by indispensable lab-related work and insufficient detection limit. For instance, molecular detection like PCR that is applied not only for detection of bacteria but also for genotyping and resistance test entails elaborate volume control, skilled pipetting and centrifugation to obtain high sensitivity and specificity, requiring expertise of lab personnel (Luo et al., 2017). LFA is vulnerable to false negatives below a bacterial concentration of about 1×10^3 CFU/mL (Huang et al., 2019), resulting in low assay sensitivity.

To overcome such challenges, we introduce here a rapid, ultrasensitive, highly accurate culture-free POCT device for detection of the pathogenic bacteria *Staphylococcus aureus* based on a 'count-on-a-cartridge' (COC) platform which minimizes complex user interventions and maximizes detection accuracy with a low detection limit. We combined a high-throughput microfluidic-based immunomagnetic concentration process using magnetic particles (MPs) conjugated with an antibody probe (Jung et al., 2019) with a cartridge capable of autonomously separating out and capturing a small number of magnetically and fluorescently labeled (using a quorum-based modified autoinducing peptide (mAIP) probe) bacteria from a great number of free unbound MPs within a passively regulated controlled time after concentration. Since a quorum-sensing inhibitor of AIP showed highly selective binding affinity toward the accessory gene regulator C (AgrC) receptor in *S. aureus* (Lyon et al., 2002), fluorescent conjugate with mAIP can be utilized as a selective probe for species-specific identification. The concentrator and COC device technologically complement each other because the cartridge acts as a medium that connects to a signal reader in a user-friendly manner. The concentrator also helps to collect bacteria in a small sample volume (~0.1 mL) in the cartridge, which enables manipulation and direct observation of bacteria at a microscopic scale. The measurements are carried out by inserting the cartridge into a compact portable fluorescent image reader and analyzing the number of fluorescently imaged bacterial cells, analogous to counting colonies on plates. Hence, the COC platform integrated with technological components from pretreatment to detection provides remarkable enhancement of bacterial count in rapidness, simplified user interface and detection accuracy comparable to standard plate counts. With the boost in speed, efficiency and recovery from the immunomagnetic concentrator, we achieved detection of *S. aureus* in 10 mL of homogenate, diluted from 1 g of raw food sample, with the concentration ranging from 100 to 10 CFU/10 mL within a couple of hours in a resource-minimal setting. Therefore, our statistical analysis assay with *S. aureus*-spiked ready-to-eat (RTE) food samples, in accordance with microbiological guidelines for RTE foods from multiple governments (FoodStandardsAustraliaNewZealand, 2018; HealthCanada, 2010) where 100 CFU per 1 g of raw food is the criteria to discern between acceptable and unacceptable, showed a detection accuracy comparable to the standard plate count method. The significance of this work is presented in Table 1.

2. Experimental procedures

2.1. Reagents and samples preparation

Conjugation of MP-SA_{ab} was carried out by affinity coating of protein A (Ø 0.5μm) (Creative Diagnostics, USA) on MPs and, subsequently, binding of the anti-*S. aureus* antibody (Abcam, USA), which is intended to bind with target bacterial cells *S. aureus* Rosenbach (ATCC25923) obtained from American Type Culture Collection (ATCC, USA). About 1.2×10^7 particles of MP-SA_{ab} were added to 10 mL homogenate for capturing and concentration. For concentration, the 10 mL post-incubated mixture of MP-SA_{ab} and homogenate was injected into the microtubular channel of the magnetic concentrator and run at flow rate of 40 mL/h by syringe pump (neMESYS, Germany), followed by collection of concentrate (0.1 mL) in the microtube. Fluorescent labeling reagent for detection was prepared with carboxylate quantum dot (QD) 525 (Thermo Fisher Scientific, USA) conjugated on mAIP synthesized and purified from JPT peptide technologies. The QD solution of 8 μM was reacted with an equimolar concentration of poly(ethylene glycol) 2-aminoethyl ether acetic acid (PEG, Sigma Aldrich, Germany) in the presence of 0.57 mg of 1-ethyl-3-[3-dimethylaminopropyl] carbodiimide (Thermo Fisher Scientific, USA) at 10 mg/mL, allowing conjugation of the QDs with the heterobifunctional PEG in 2 hrs of incubation at room temperature. The QD-PEG reactant was filtered through a 0.2 μm syringe filter and column chromatography (Econo-Pac 10DG column, Bio Rad, Hercules, CA) for purification. Then, the mAIP was reacted with the QD-PEG for conjugation by repeating the protocol applied to synthesize the QD-PEG. 40 nM of QD-mAIP was added and incubated with the 0.1 mL concentrate. Tryptic soy broth (TSB) and Baird-Parker agar (BPA) for bacterial growth were purchased from Difco (UK) and egg yolk tellurite emulsion was acquired from Oxoid (UK). The analytical profile index (API) kit for biochemical identification of bacteria was purchased from bioMérieux (France). 1× phosphate-buffered saline (PBS) supplemented with 0.1% Tween 20 and 2% bovine serum albumin purchased from Sigma Aldrich was used for diluents and wash buffer.

2.2. Materials, design and manufacture of sensing cartridge

The following materials were used for the cartridge: CF6 and CF7 absorption pads (Whatman, USA), water-soluble tape (SUNfabric, Korea), injection-molded plastic components for the polycarbonate (PC) plate and black acrylonitrile-butadien-styrene (ABS) cases (Dae-jin plastic, Korea). A custom-built stainless puncher was used for manufacturable tailoring of absorption and water-soluble tape. A 3D printer (M50, MiiCraft, Taiwan) was used for building a jig that helps precise mounting of water-soluble tape on the PC plate. For functional hydration of the water-soluble tape, a compact ultrasonic humidifier as a consumer electronics (0.5 L capacity) was hermetically tubed with a Ø 8-mm tube for puffing out moisture in the center of the mounted water-soluble tape. Glycerol (99.9%, Sigma Aldrich) was diluted to 80% and 30 μL of the solution was pre-filled in the incubating space of the cartridge before sample input. The incubating space was designed to have a high aspect ratio that contains ~130 μL of volume with the tight base conformable to the microscopic field of view (FOV) of 1.45 mm × 1.73 mm (width × length).

2.3. Hardware and software design of fluorescent image reader

The fluorescent microscopic module was obtained from f1 single compact microscope (Nanoscope Systems, Korea) to rebuild and customize the fluorescent image reader. At the side of the reader, a cartridge loading slot for insertion was guided with a fixed rail for precise in and out movement as well as the location where the region of the interest (ROI) to be focused in the incubation space of the cartridge is

Table 1
Significance of this work in comparison with the recently published reports for the detection of bacterial pathogens.

Test method	COC	Colorimetry on LFA	PCR with hand-powered nucleic acid isolation	Impedimetry in microfluidic device
Detection target	*Staphylococcus aureus*	*Listeria monocytogenes*	*Brucella ovis*	*Salmonella typhimurium*
User-convenience	High	High	Low	High
Total assay time (preparation and detection) over 10 mL sample	77 min	>8 hrs	60 min	60 min
Limit of detection	1 CFU/mL	53 cells/mL	1 CFU/mL	300 cells/mL
Diagnostic accuracy with low cut-off value (100 CFU/10 mL)	AUC: 0.985	N/A	N/A	N/A
Reference	This work	Tasbasi et al. (2019)	Zhao et al. (2019)	Liu et al. (2019)

pre-defined and center aligned with the microscope for reliable image acquisition in repeated tests. For the electronic control optical module, electronic components and parts were purchased from Hardkernel (Korea). A circuit was designed by KiCad and prototyped for control board as a minicomputer by utilizing ODROID XU4 wired to a touch screen module, light emitting diode (LED) and complementary metal-oxide semiconductor (CMOS) camera with inter-components optimization for the device operation of fluorescent image acquisition, image processing and result report. A Linux-based application software algorithm of image processing for fluorescent bacteria counting was written with OpenCV 3.4.1 library. Implementation of the image processing algorithm follows the procedure described below.

2.3.1. Capture

A fluorescent image is captured by the camera mounted on the microscope. In the capture process, the captured image consists of 24-bit RGB 3 channels; an 8-bit green channel is used in this paper because the spectral response of the green channel contains most of the wavelength of the fluorescent light.

2.3.2. Noise filtering

In the capture process, the dark noise (Nakamura, 2005) by the electrical characteristic on the image sensor causes random noise in the captured image. This can affect the counting algorithm and minimization of the noise is necessary. Here, a bilateral filter (Tomasi and Manduchi, 1998) is applied to the image to minimize the random noise.

2.3.3. Binarization

After noise filtering, the noise in the image is minimized and only the fluorescent dots remain. To discriminate the region of fluorescent dots and background, the binarization process changes the pixel value to 0 or 1 according to the empirically selected threshold level. The binarized pixel value is set to 1 if the corresponding image pixel level is higher than the threshold, otherwise the binarized pixel value is set to 0. After the binarization process, the binarized image contains two levels of pixel values (1 and 0) and each value represents the region of fluorescent dots and background, respectively.

2.3.4. Boundary detection

The boundary detection of each fluorescent dot is necessary to check its size and the number of bacteria. In this paper, the Suzuki and Abe (Suzuki and be 1985) boundary detection algorithm was applied to the binarized image. After the boundary detection process, the pixel positions of each boundary are stored, and can be used to count the number of fluorescent dots which represent the place of bacteria.

2.3.5. Bacteria counting

In this paper, the number of bacteria was calculated by the summation of the number of fluorescent dots in the binary image with the boundary detection method. In certain cases, several fluorescent dots can overlap, and the boundary detection algorithm recognizes this as a single dot. To count the overlapped dots correctly, the size of each boundary was also calculated by accumulating the number of pixels inside each boundary, respectively. In the middle of the counting method, each boundary size is divided by the pre-defined unit boundary size and the result should be 1 if the boundary size is similar to unit size. In overlapped boundary cases, the result should be the same as the number of dots in the overlapped boundary because its size is bigger than the unit boundary size. In this manner, the total number of bacteria can be counted as follows: $F = \{F_1, F_2, ..., F_K\}$ is the set of each fluorescent dot in the image, and K is the number of dots. Each fluorescent dot can be defined by the set $F_i = \{(x_{i1}, y_{i1}), (x_{i2}, y_{i2}), ..., (x_{iJ}, y_{iJ})\}$, where i is the index of the corresponding dot and (x_{ij}, y_{ij}) is the pixel position index at the place of the ith dot. j is the number of pixels in the set F_i. If there are the arbitrary set F_i and F_j, $F_i \cap F_j = \varnothing$ is satisfied. Finally, total number of bacteria can be calculated by $(\text{total number of bacteria}) = \sum_{i=1}^{K} \left\lceil \frac{|F_i|}{f_{unit}} \right\rceil$, where $|F_i|$is the cardinality of the set F_i, and $f_{unit}$is the coefficient of pre-defined unit size which can be determined by empirical measurement of fluorescent dot size. $\lceil \cdot \rceil$ is the ceiling operator.

2.4. Preparation of spiking samples

For the quantitative assay, *S. aureus* were grown in 100 mL of TSB up to the mid-exponential growth phase, reaching an OD_{600} of 100 μL to 0.05, and 1 mL aliquots of bacteria containing 1×10^7 CFU were diluted to desired spiking levels. 1 g of RTE tofu salad mixed with 9 mL diluent was homogenized by a stomacher (BNF KOREA, Korea) in a Whirl-Pak bag (Nasco, USA) and collected after filtration inside the bag. Spiking bacteria were then added to the 10 mL homogenate. The actual bacterial number at the desired spiking level was confirmed by plate counts on BPA agar plate and decided by average in triplicate while operating the COC device with the same spiking levels. For the selectivity test, *E. coli* (ATCC8739) and *S. enterica* (ATCC13311) were separately cultured on nutrient agar (Difco) plate and a colony of each strain was taken and serially diluted 10-fold with 3 times for spiking and use.

2.5. Statistical analysis of assay results

For every run of the COC assay with spiked samples, the detection results reported on the screen of the fluorescent image reader were recorded, compiled into Excel (Microsoft, USA) and compared to the result from plate counts in triplicate with the same spiking levels of the tested samples. SPSS (IBM, USA) and MedCalc (MedCalc Software, Belgium) were used for Passing-Bablok regression and Bland-Altman plot, respectively, with a confidence interval (CI) of 95%. ROC curve analysis as well as calculation for sensitivity and specificity of the assay was carried out.

2.6. Sample preparation and characterization with electron microscopy

The reagents used in preparation for electron microscope imaging were purchased from Sigma Aldrich. For field-emission scanning

electron microscope (FE-SEM) (JEOL, Model JSM-6500F, Japan) imaging of MP-SA_{ab}-*S. aureus* complex, the magnetic concentrate was placed on nitrocellulose mixed ester membrane filter with the pore size of 0.2 μm (STERLITECH, USA) after fixation in the 2% glutaraldehyde mixed 1× PBS solution with pH 7.4 for 30 min at room temperature. 30%, 50%, 70%, 90% and 100% ethanol were placed in turn for dehydration, followed by overnight air-drying. For transmission electron microscope (TEM) (FEI, Talos L120C, Czech) imaging of the complex of MP-SA_{ab}-*S. aureus*-QD-mAIP, the magnetic concentrate reacted with QD-mAIP was fixed and dehydrated in the 1 mL microtube using the same reagents for SEM imaging. At the each step, the centrifugation of 5000 rpm for 10 min was implemented for pelleting the sample. After dehydration, ethanol inside the sample had transition to propylene oxide and the sample was embedded in spurr's resin, followed by overnight polymerization at 70 °C. The polymerized stick with the sample at the tip was sliced in 100 nm thickness by using ultramicrotome (Leica, EM UC7, Germany).

3. Results and discussion

3.1. Testing procedure and advantages of the count-on-a-cartridge platform for assays of food-borne bacteria

Typical food-borne bacteria detection in quantification mode requires inoculation of diluted homogenate sample on laboriously prepared agar plates, an incubation period of over a day and further tedious labor-intensive identification with additional incubation, which is carried out over several days (Fig. 1A). The workflow of our newly developed bacterial COC assay is shown in Fig. 1B. The whole volume of 10 mL homogenate prepared from stomaching of tofu salad spiked with *S. aureus* is mixed with MP-*S. aureus* antibody (MP-SA_{ab}), prepared according to the scheme in Fig. 1C for magnetic capture and concentration of *S. aureus*, for 40 min. Then, the 10 mL mixture of MP-SA_{ab} and unbound free MPs is concentrated to 0.1 mL (15 min) for introduction into the cartridge. For selective detection and species-specific identification, a green-emitting quantum dot (QD) conjugated with mAIP (QD-mAIP) (Fig. 1D), which is specifically bound to AgrC, a membrane-bound histidine kinase, on the cell wall of pathogenic *S. aureus* for fluorescence labeling (Fig. 1E) is mixed with MP-SA_{ab} concentrate (15 min). This is then transferred to the sensing cartridge, and MP-SA_{ab} bound with QD-mAIP is autonomously separated from free MPs using the pre-filled high-viscosity glycerol solution within a self-terminating incubation time (15 min). Finally, the incubation-terminated cartridge is inserted into the cartridge loading slot in a fluorescent image reader and the reader reports the count of fluorescent bacterial cells held by a hard magnet within the field of view on the cartridge via algorithm-processed image analysis (2 min).

Due to the concentrator device configuration, in which vertically-wound microtubular fluidic channels integrated with magnetic manipulation give the bacteria a quick ride in the concentrating step (Jung et al., 2019) and the sensing cartridge removes a great number of unbound MPs, leaving the bacterial cells which are bound with QD-mAIP probes for fluorescence imaging and quick passive counting of bacteria cells, a total test time for sample-to-answer within 2 h is possible with minimal user-intervention and use of lab instruments. Imaging of sectioned complex of bacterial cell with MP-SA_{ab} and QD-mAIP characterized by transmission electron microscopy indicates the binding of QD-mAIP and MP-SA_{ab} on the surface of bacterial cell (Fig. 1F).

3.2. Development and testing of the count-on-a-cartridge (COC) platform

Disposability, reliability and user convenience were primarily considered for development of the bacterial COC for its on-site operation. The design of the cartridge was based on the use of low-cost materials and reliability of the end product. The materials used for the cartridge are listed in Fig. 2A. Briefly, the cartridge is assembled by putting a cylinder magnet of 1 mm × 1 mm (diameter × height) in the fitting space between the bottom case and transparent polycarbonate (PC) plate (2.5 cm × 2.5 cm) where water soluble tape with a center hole (h_1) is axially attached on the plate and above it an absorption pad with a center hole (h_2) ($h_2 > h_1$ in diameter) is aligned through the top and bottom case. Plastic components such as the PC plate and cartridge case were produced by an injection molding method, resulting in a total cost of USD 0.5 per unit, robustness of performance, and manufacturability. Previously developed user-friendly cartridge concepts (Lee et al., 2019) have been enhanced in this work in terms of lab-less functionality, which provides not only a self-terminating incubation time but also passive removal of unbound MPs through magnetophoresis in a high-viscosity glycerol solution.

To facilitate magnetophoretic removal of free MPs for successful imaging of bacterial cells, it is important that the glycerol solution be controllable like water within a certain time for separation of magnetically and fluorescently labeled *S. aureus* cells from free MPs on the cartridge. Pristine water-soluble tape, the key material for passive control of sample incubation time in the cartridge, is responsive only to water and not to the glycerol solution for 20 min. This is because the capillary action of water (lower viscosity) occurs easily through disintegration of the tape material but the glycerol solution (much higher viscosity) can hardly get through the material by capillary action, as explained by other literature (O'Loughlin et al., 2013; Washburn, 1921). A way for the glycerol solution to traverse the tape within 15 min is to create bigger capillaries on the surface of the material so that the capillary flow velocity can be dramatically increased. Fig. 2B shows the process of creating bigger capillaries. The water soluble tape with h_1 attached and aligned at the center of the PC plate in the cartridge is hydrated with a humidifier to disintegrate its tissue, followed by overnight drying for the completion of microchannel formation, which is confirmed in before-and-after microscope images in Fig. S1.

Since passive control of the glycerol solution is possible, the cartridge can utilize the vertically applied magnetic attraction that separates MP-SA_{ab} from free MPs in the glycerol layer during the incubation between finishing (t_{finish}) and starting time (t_0), as well as drain unbound MPs from the area above the hard magnet in the chamber of the cartridge, as shown in Fig. 2C. Tests with three reliably working cartridges proved the drainage of the contents after the self-terminating incubation time (Fig. 2D). To reveal the fluorescently labeled MP-SA_{ab} attracted by the bottom magnet and captured on the surface of PC plate, the optimum load of MPs that has maximum throughput for the removal capacity of free MPs was empirically optimized. Otherwise, the fluorescent bacteria cells are buried in the greater number of free MPs and the fluorescent signal is lost. Removal efficiency of free MPs is strongly dependent upon capillary wicking rate of the absorption pad. With the amount of MPs used for concentrating 10 mL homogenate sample to 0.1 mL concentrate, an absorption pad with a wicking rate of 35 s/4 cm (where the rate is expressed as the time for liquid to move through 4 cm of the material) showed the best performance for the removal of free MPs (Fig. S2). Notably, in the necessity of changing wicking rate according to different load or size of MPs, an absorption pad with different porosity that affects capillary capacity would be selected by considering needs for manipulation of the wicking rate. After washing the fluorophore residue by drips of washing buffer, fluorescent *S. aureus* cells are ready to be counted with fluorescent imaging as if colony counting on agar plates, sheathed by a 0.3-mm-deep trench with a diameter of 1.5 mm at the center of PC plate (Fig. 2E). The selectivity was confirmed with the detection tests by adding Gram-negative bacterial strains such as *E. coli* and *S. enterica* to *S. aureus* (Fig. S3). In the case of detecting other bacterial strains, the optimization according to specific strain is required and it would include the selection of an antibody as a capture probe and a selective fluorescent labeling molecule as a detection probe.

By integrating complex functions in the sensing cartridge that are passively operative, handling of the testing workflow is enhanced in a user-friendly manner. Otherwise, steps like sample incubation and

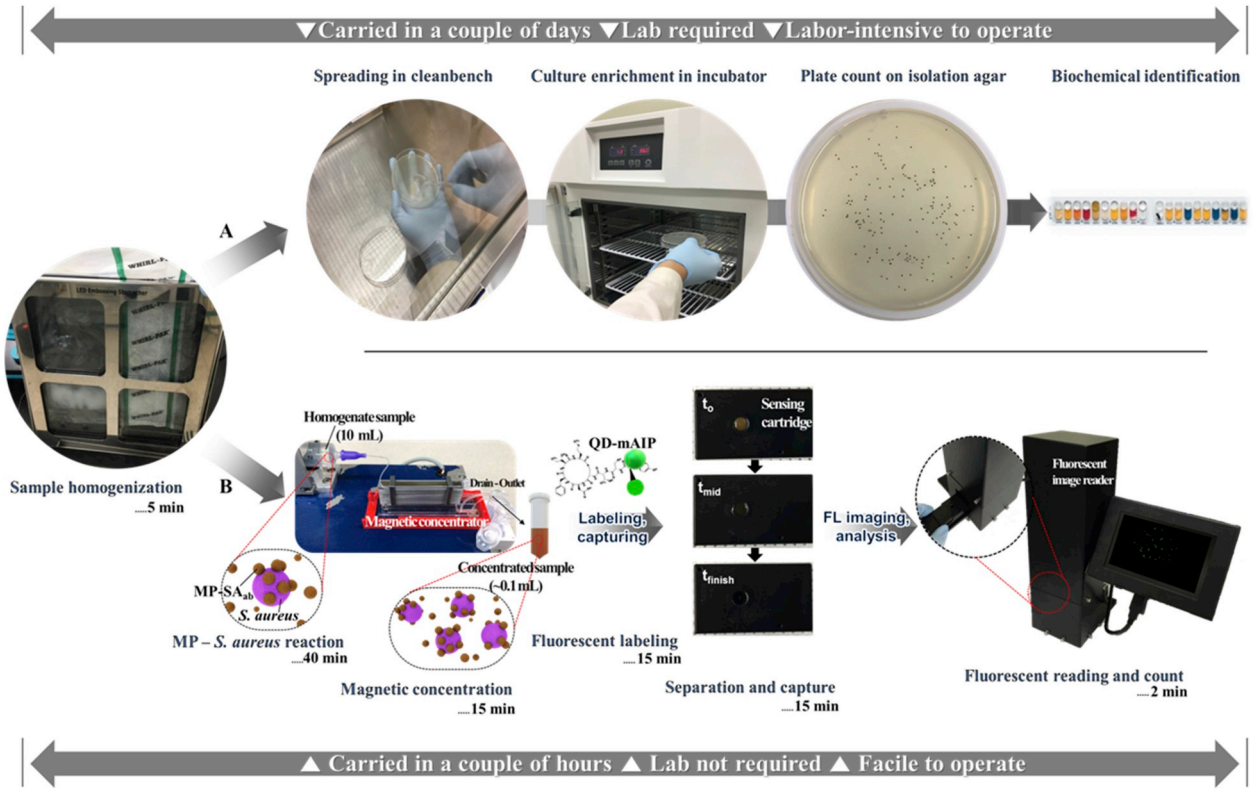

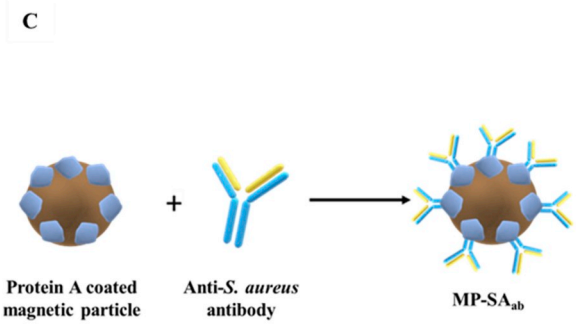

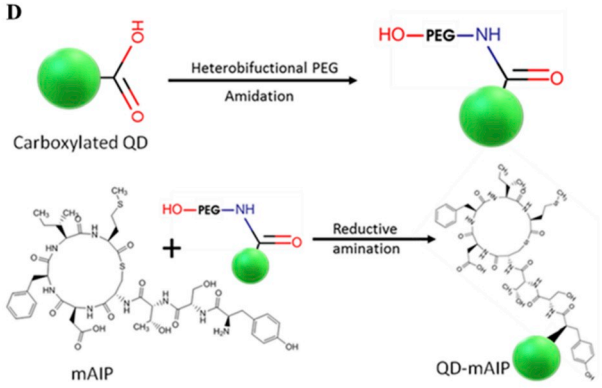

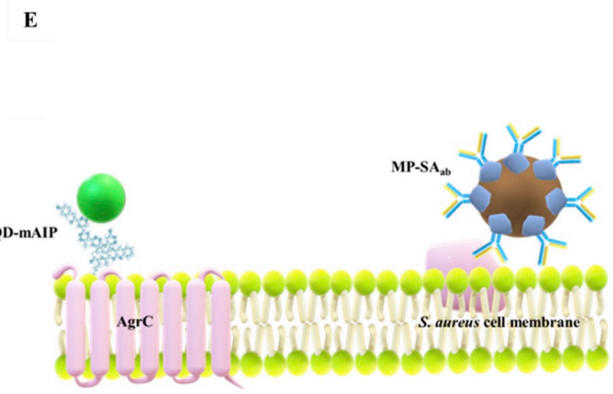

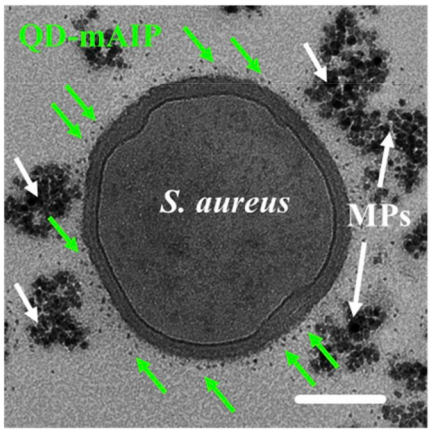

(caption on next page)

Fig. 1. Comparison of the assay flow for selective bacteria detection between the conventional method and the count-on-a-cartridge assay with magnetic and fluorescent probes. (**A**) The quantitative plate count, the gold standard, for bacteria detection. The homogenate is placed on a selective agar plate and incubated overnight for bacterial growth and colony visibility. Preparation of culture medium and spreading the sample on the plate is labor-intensive and must take place in a lab environment with a clean bench and incubator. (**B**) Homogenate sample mixed with MP-SA_{ab} is transferred to the microbial magnetic concentrator and concentrated to a low volume for the count-on-a-cartridge assay. QD-mAIP is loaded in the bacterial concentrate for highly specific fluorescent labeling and identification of *S. aureus*. Labeled bacterial concentrate is introduced into the sensing cartridge with pre-filled glycerol where free MPs are passively removed in a self-terminating time, leaving MP-*S. aureus*-QD captured on the sensor surface. After dropping 10 μL of washing buffer, the user inserts the cartridge into the loading slot in the fluorescent image reader for fluorescent image acquisition and analysis of quantitative counts of fluorescent *S. aureus*. The whole process is finished in less than 2 h and the user can transfer samples by pipetting without lab tools like a clean bench or incubator. (**C**) Protein A coated MPs were attached with the anti-*S. aureus* antibody to synthesize MP-SA_{ab}. (**D**) The mAIP probe was conjugated with QD using heterobifunctional polyethylene glycol (PEG) to obtain QD-mAIP. (**E**) QD-mAIP specifically binds to accessory gene regulator C (AgrC) receptor expressed in the cell membrane while SA_{ab} binds to the surface of *S. aureus* cells. (**F**) 100-nm-thick section of the complex of *S. aureus* conjugated with MP-SA_{ab} (white arrow) and QD-mAIP (green arrow) was characterized by transmission electron microscopy. The scale bar is 200 nm. (For interpretation of the references to colour in this figure legend, the reader is referred to the Web version of this article.)

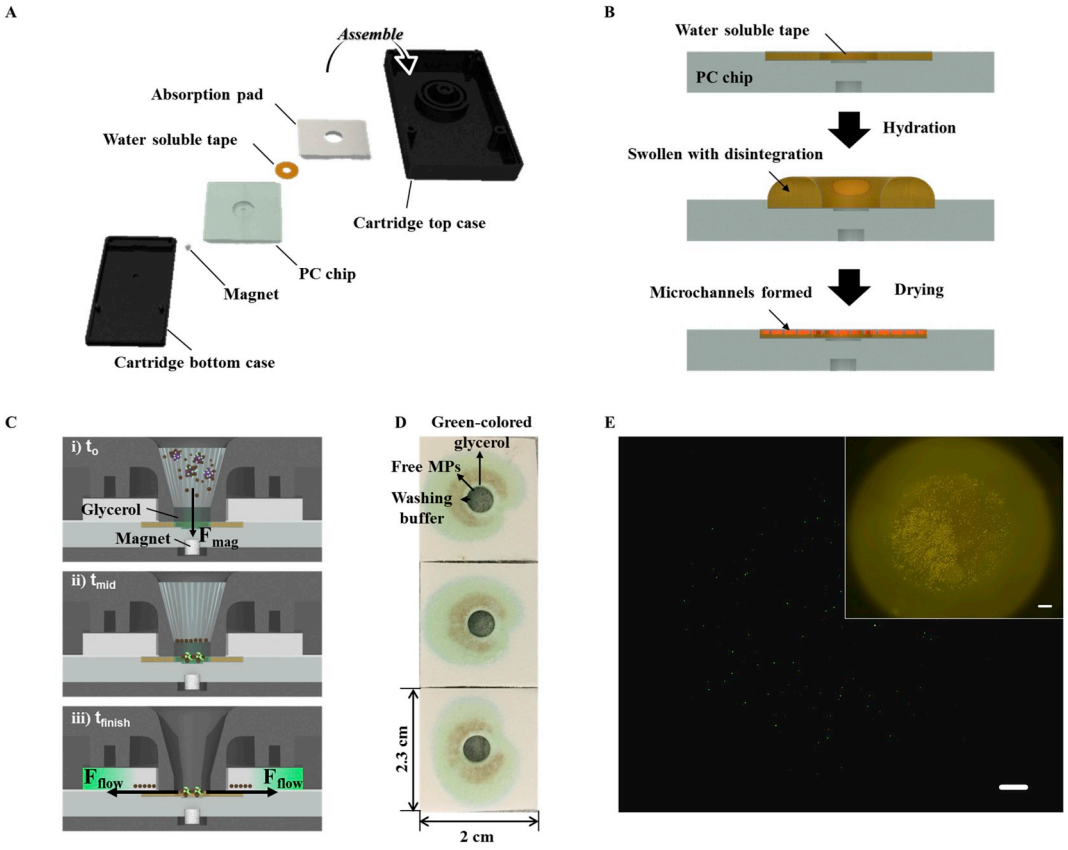

Fig. 2. Development and testing of the count-on-a-cartridge platform. (**A**) 3D visualization of material components of the cartridge. (**B**) Procedure to form microchannels for the highly viscous glycerol solution to facilitate capillary action. (**C**) Autonomous operation to control self-terminating incubation time for separation of magnetically and fluorescent labeled *S. aureus* from free MPs on the cartridge. i) - ii) Vertical magnetic attraction of magnetically and fluorescent labeled *S. aureus* for separation from free MPs during t_{finish} - t_0. iii) Horizontal flow force draining all contents outwards leaving captured fluorescent *S. aureus* at t_{finish}. (**D**) Image of absorption pads of three devices after time of termination in series that shows working reliability. (**E**) Fluorescent image shows that fluorescent *S. aureus* cells are ready for counting on the surface of cartridge. The inset is the same view imaged in bright field mode. The scale bar is 100 μm.

particle separation would require labor-intensive, hands-on lab work such as repetitive pipetting and centrifugation.

3.3. Set-up of the fluorescent image reader

The custom-built fluorescent image reader was made of a compact fluorescent microscope module (100× magnification) with a CMOS image sensor (CIS) digital camera with a blue LED as a light source (wavelength of 465 nm), electronics for system control, loading slot for cartridge insertion, housing with a black metal case 30 cm × 10 cm × 10 cm (height × width × depth) and a touch screen with a computing module at the side that is connected to the camera and wired to the power supply. Further information on the hardware is shown in Fig. S4. All the hardware components used for building fluorescent image reader and integrated COC testing platform are listed in Table S1. The cartridge is inserted into the loading slot (left panel, Fig. 3A). The trench with a diameter of 1.5 mm on the cartridge is focused in the microscopic FOV and imaged in fluorescent mode (λ_{ex} = 460 nm, λ_{em} = 525 nm) with a bandpass filter of 525/10 nm. Fig. 3B shows how the fluorescent image of the bacteria cells is analyzed to count the number of bacteria by applying a built-in image processing algorithm that includes noise filtering, binarization, boundary detection and size-distinguishable bacteria counting. The description in Fig. S5 helps to clarify the methods for the imaging processing algorithm for bacteria cell counting. As designed in the user interface (UI) state diagram (Fig. S6), the analysis software was built for the user to operate the detection procedure (Fig. 3C). After insertion of the cartridge into the reader, the user taps the 'Bacteria measurement' menu and then the 'capture' menu to take a

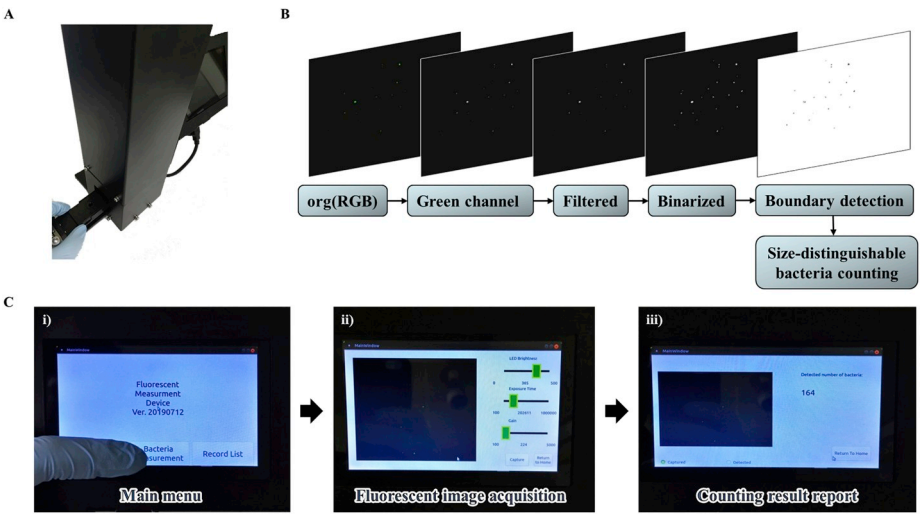

Fig. 3. Acquisition step of detection signal for the count-on-a-cartridge assay. (**A**) Insertion of the incubation-terminated cartridge into the loading slot of the fluorescent image reader. (**B**) The procedure of a series of image processing algorithms applied on the taken image for fluorescent bacteria counting. (**C**) Photograph of the detection operation. i) User taps "Bacteria measurement" at the Main menu on the touch screen. ii) User acquires a fluorescent image with preset configurations such as light power output, camera exposure time and signal gain by tapping "Capture". iii) Counted bacterial number is reported and displayed with the raw fluorescent bacteria image after processing image by the embedded algorithm.

fluorescent image with preset optical settings such as light source output, exposure time and signal gain to process the analytic algorithm, followed by the result report for the bacterial count on the screen. Fluorescent images for the quantification report of COC detection results with high and low spiking levels are visualized in Fig. S7.

3.4. Statistical characterization and accuracy test of count-on-a-cartridge platform using a homogenized food sample in comparison with the plate count method

For performance characterization of the bacterial detection assay from a raw food sample based on the COC platform by combining immunoconcentration of its homogenates (Fig. S8), the recovery rate of bacteria from the magnetic concentrator in the lower range of bacterial spiking concentration was first confirmed. This is required for determination of recovery rate in the front-end of the system, magnetic concentrator-to-sensing cartridge, and application of the system for practical use for *S. aureus* detection in accordance with global criteria for RTE food, which is 100 CFU per 1 g of raw sample. In light of homogenization that is proceeded with 10 times dilution per input of raw sample, the bacterial spiking was prepared in a total volume of 10 mL of homogenized food sample (9 mL diluent with 1 g raw food sample). Three different spiking samples in 10 mL were concentrated to 0.1 mL with the magnetic concentrator and then plate-cultured in triplicate. As summarized in Fig. 4A and Table S2, the results confirmed that the average count difference between before- and after-magnetic concentration is 9 to 10 on average at low spiking levels, 67, 103 and 182 CFU/10 mL, resulting in a recovery rate of 85%, 91.2% and 94.7% with relative standard deviations (RSD) of 8.7%, 6.5% and 2.3%, respectively. The latter part of the system, the sensing cartridge-to-fluorescent image reader, was characterized with statistical validation of the cartridge if the self-terminating incubation time and bacterial recovery at low spiking levels are reliable. After testing 26 cartridges with *S. aureus*-spiked food samples of 0.1 mL concentrated with the magnetic concentrator from a 10 mL volume containing 110 cells, we found that the self-termination time is on average 805 s with a standard deviation of 75 s and a RSD of 9.3%. The recovery rate of the whole process of the COC assay was consistently measured as 91.1% with RSD of 2.4% on average over cartridge operations (Fig. 4B and Table S3).

We conducted statistical analytical assays and accuracy tests for 44 different *S. aureus*-spiked samples with an initial homogenate volume of 10 mL, which were prepared as described in the experimental section, in order to assess whether the analytical performance of the COC platform is comparable to that of the conventional plate count method. Table S4 shows the statistical analytical assay data from both methods, verifying the recovery rate at each spiking level. Based on the detection results, very close agreement between the two methods was observed in the Passing-Bablok (Passing and Bablok, 1983) and Bland-Altman (Martin Bland and Altman, 1986) analysis presented in Fig. 4C and D, respectively. In the Passing-Bablok analysis, the results showed an intercept A value of -9.51 as systematic differences with a 95% confidence interval (CI) of -12.13 to -9 and a slope B value of 1.014 as proportional differences with a 95% CI of 1 to 1.04 (Fig. 4C). The cumulative sums (CUSUM) test for linearity indicated no significant deviation from linearity with $P > 0.05$, where a P value in the CUSUM test less than 0.05 indicates significant difference from linearity between two sets of data, which is not suitable for a conclusion on agreement between two methods (Bilić-Zulle, 2011). The Bland-Altman analysis presented a mean difference of -8.7, within the limit of agreement, which is defined as the mean difference plus or minus 1.96 times the standard deviation of the differences in comparison (Fig. 4D). The accuracy of the COC assay for the whole testing procedure from homogenate sample to concentration to detection was evaluated with the cut-off value of 100 CFU/10 mL (homogenate sample), judging true or false diagnosis by detection results of plate counts with the samples with the same *S. aureus* spiking levels with observance of the criteria of 100 CFU/1 g (raw sample). On the interactive plot shown in Fig. 4E, finding two false-negatives, the sensitivity and specificity of COC assay were 92.9% and 100%, respectively. Based on the receiver operating characteristic (ROC) curve analysis, the obtained area under ROC curve (AUC) was 0.985 for the COC assay (Fig. 4F), which indicates accurate diagnosis and high comparability with the standard plate count method in accordance with global food criteria for food-borne *S. aureus*.

The recovery rate throughout consecutive stages of concentration and COC detection, which can be caused by undesired loss of bacterial cells from the original number, affected false negatives. The proven recovery rate of the bacteria over the whole COC assay from 10 mL of bulk homogenate (homogenized from 1 g of food sample) to microscopic FOV on the cartridge, guided by magnetic manipulation and identified by fluorescent marks, necessarily secured the detection accuracy in the setting of the same cut-off value as the global criteria. Furthermore, the COC assay achieved quantitative, identifiable and species-specific detection of bacteria at much lower spiking levels than the cut-off, down to 10 CFU per 10 mL (1 CFU/mL), with a compromised recovery rate of 10% (Table S4). The outcome envisioned that precise magnetic control of bacterial collection with advanced imaging engineering providing the imaging capability of a single bacterial cell can contribute to accurately monitor extremely low levels of *S. aureus*. Further efforts to improve the recovery rate of bacteria during a series of steps including capturing, concentrating and detecting bacteria from the raw food

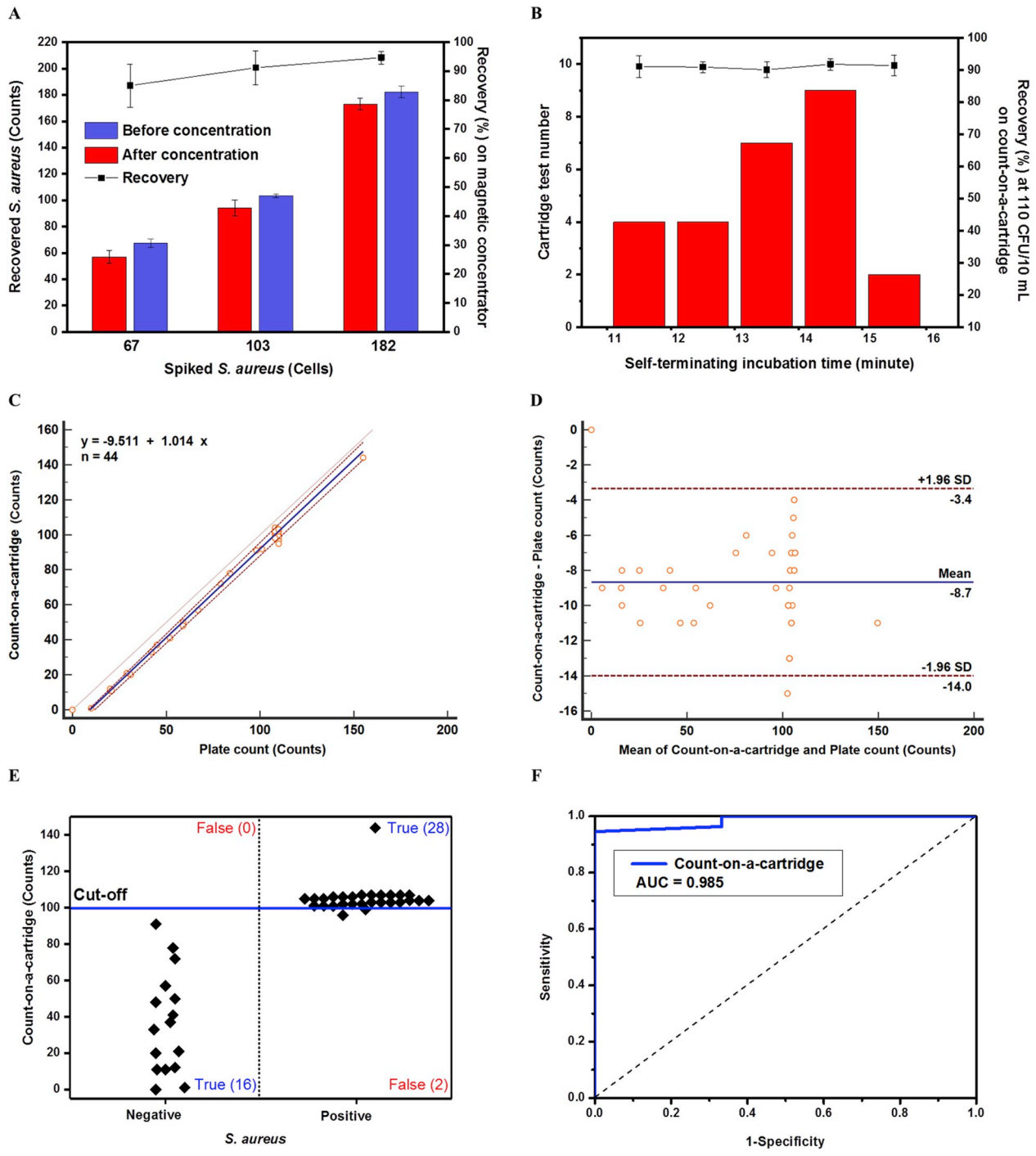

Fig. 4. Assessment of recovery rate on the count-on-a-cartridge device with *S. aureus*-spiked food samples, followed by detection performance of count-on-a-cartridge assay compared to plate count method with 44 spiked food samples. (**A**) Recovery performance of the front-end of the system, magnetic concentrator-to-sensing cartridge, at low spiking level at three points was comparatively confirmed between before- and after-concentration of bacterial cells in the homogenate sample volume of 10 mL by plate count method. (**B**) Self-terminating incubation time was characterized and the bacterial recovery rate from the magnetic concentration-to-fluorescent image reader at the same spiking level (110 CFU) in the homogenate volume of 10 mL was also confirmed with tests of 26 cartridges. (**C**) Passing-Bablok analysis of the detection results measured by COC assay and plate count method. The center dashed line represents the regression line, blue solid line indicates the identity and two dashed lines show the confidence interval. (**D**) Bland-Altman analysis of the detection results measured by COC device and plate count method. The blue solid line indicates the mean difference of the two methods and two dashed lines represent the 95% limit of agreements. (**E**) The interactive plot shows the detection results of the COC device distributed in negative and positive groups in accordance with cut-off value. The cut-off value was set at 100 CFUs in the homogenate sample of 10 mL (observance of criteria 100 CFU/1 g in raw food sample). (**F**) Receiver operating characteristic (ROC) curve with area under ROC curve (AUC) of 0.985 for the statistical assay results of the COC device is shown.

matrix can possibly increase the specificity of the assay by minimizing false negatives.

4. Conclusions

The COC assay platform demonstrates a novel approach for POCT of *S. aureus* that is carried out culture-independently within a couple of hours and gives highly sensitive and accurate enumeration comparable to the conventional plate count method. The assay platform gives a quick method for bacteria to be collected in smaller volume from a large volume of homogenate and reduces assay time from a couple of days to a couple of hours with a simple and species-specific fluorescent identification based on the quorum-sensing system of the bacteria. The high recovery rate of the bacteria from bulk homogenate sample to microscopic FOV on the cartridge greatly contributes to minimization of false signals and, in turn, gives statistically accurate results. Furthermore, passive handling of concentrated bacteria on the cartridge as well as signal readout using a portable fluorescent imager for direct observation of fluorescent bacterial cells provide great improvements in user convenience. The potential reach of our work could be extended from food to blood samples where time between recognition and decision to treat for infection needs to be shortened, being attractive for a wide range of applications in resource-constrained or urgent situations.

Declaration of competing interest

The authors declare that they have no known competing financial interests or personal relationships that could have appeared to influence the work reported in this paper.

CRediT authorship contribution statement

Won-Il Lee: Methodology, Investigation, Validation, Data curation, Writing - original draft. **Younghyeon Park:** Software, Methodology. **Sajal Shrivastava:** Methodology, Resources. **Taekeon Jung:** Resources. **Montri Meeseepong:** Resources. **Jaelin Lee:** Resources. **Byeungwoo Jeon:** Project administration. **Sung Yang:** Project administration. **Nae-Eung Lee:** Conceptualization, Funding acquisition, Supervision, Writing - review & editing.

Acknowledgments

This research was supported by the Nano Material Technology Development Program (NRF-2016M3A7B4910554) through the National Research Foundation of Korea (NRF) funded by the Ministry of Science and ICT and also by Basic Science Research Program (No. 2019R1A6A1A03033215) and Global PhD Fellowship Program (NRF-2015H1A2A1034159) through the National Research Foundation of Korea (NRF) by the Ministry of Education.

Appendix A. Supplementary data

Supplementary data to this article can be found online at https://doi.org/10.1016/j.bios.2020.112007.

References

Bilić-Zulle, L., 2011. Biochem. Med. 21 (1), 49.
Chaivisuthangkura, P., Pengsuk, C., Longyant, S., Sithigorngul, P., 2013. J. Microbiol. Methods 95 (2), 304–311.
Chen, J., Shi, X., Gehring, A.G., Paoli, G.C., 2014. Int. J. Food Microbiol. 179, 33–37.
Chen, J., Tang, J., Liu, J., Cai, Z., Bai, X., 2012. J. Appl. Microbiol. 112 (4), 823–830.
FoodStandardsAustraliaNewZealand, 2018.
Fukushima, H., Katsube, K., Hata, Y., Kishi, R., Fujiwara, S., 2007. Appl. Environ. Microbiol. 73 (1), 92.
Goldmeyer, J., Li, H., McCormac, M., Cook, S., Stratton, C., Lemieux, B., Kong, H., Tang, W., Tang, Y.-W., 2008. J. Clin. Microbiol. 46 (4), 1534.
HealthCanada, 2010.
Hessling, M., Feiertag, J., Hoene, K., 2017. Biosc. Biotech. Res. Comm. 3 (10).
Huang, Z., Peng, J., Han, J., Zhang, G., Huang, Y., Duan, M., Liu, D., Xiong, Y., Xia, S., Lai, W., 2019. Food Chem. 276, 333–341.
Joshi, R., Janagama, H., Dwivedi, H.P., Senthil Kumar, T.M.A., Jaykus, L.-A., Schefers, J., Sreevatsan, S., 2009. Mol. Cell. Probes 23 (1), 20–28.
Jung, T., Jung, Y., Ahn, J., Yang, S., 2019. submitted for publication.
Kim, H.J., Kwon, C., Lee, B.S., Noh, H., 2019. Analyst 144 (7), 2248–2255.
Lee, W.-I., Park, Y., Park, J., Shrivastava, S., Son, Y.-M., Choi, H.-J., Lee, J., Jeon, B., Lee, H., Lee, N.-E., 2019. Lab Chip 19 (8), 1502–1511.
Li, Q., Zhang, S., Cai, Y., Yang, Y., Hu, F., Liu, X., He, X., 2017. Int. J. Food Sci. Technol. 52 (7), 1559–1566.
Li, X., Ximenes, E., Amalaradjou, M.A.R., Vibbert, H.B., Foster, K., Jones, J., Liu, X., Bhunia, A.K., Ladisch, M.R., 2013. Appl. Environ. Microbiol. 79 (22), 7048.
Liu, J., Jasim, I., Shen, Z., Zhao, L., Dweik, M., Zhang, S., Almasri, M., 2019. PLoS One 14 (5), e0216873.
Luo, D., Huang, X., Mao, Y., Chen, C., Li, F., Xu, H., Xiong, Y., 2017. J. Dairy Sci. 100 (10), 7883–7890.
Lyon, G.J., Wright, J.S., Muir, T.W., Novick, R.P., 2002. Biochemistry 41 (31), 10095–10104.
Mao, Y., Huang, X., Xiong, S., Xu, H., Aguilar, Z.P., Xiong, Y., 2016. Food Control 59, 601–608.
Martin Bland, J., Altman, D., 1986. Lancet 327 (8476), 307–310.
Nakamura, J., 2005, first ed. CRC Press.
Nezhad, A.S., 2014. Lab Chip 14 (16), 2887–2904.
O'Loughlin, M., Wilk, K., Priest, C., Ralston, J., Popescu, M.N., 2013. J. Colloid Interface Sci. 411, 257–264.
Passing, H., Bablok, W., 1983. Clin. Chem. Lab. Med. 21 (11), 709–720.
Poshtiban, S., Javed, M.A., Arutyunov, D., Singh, A., Banting, G., Szymanski, C.M., Evoy, S., 2013. Analyst 138 (19), 5619–5626.
Puttaswamy, S., Lee, B.D., Sengupta, S., 2011. J. Clin. Microbiol. 49 (6), 2286.
Reddy, B., Hassan, U., Seymour, C., Angus, D.C., Isbell, T.S., White, K., Weir, W., Yeh, L., Vincent, A., Bashir, R., 2018. Nat. Biomed. Eng. 2 (9), 640–648.
Ryu, J., Park, S.H., Yeom, Y.S., Shrivastav, A., Lee, S.-H., Kim, Y.-R., Kim, H.-Y., 2013. Food Control 32 (2), 659–664.
Stewart, L.D., Tort, N., Meakin, P., Argudo, J.M., Nzuma, R., Reid, N., Delahay, R.J., Ashford, R., Montgomery, W.I., Grant, I.R., 2017. BMC Vet. Res. 13 (1), 131.
Suzuki, S., be, K., 1985. Comput. Vis. Graph Image Process 30 (1), 32–46.
Tasbasi, B.B., Guner, B.C., Sudagidan, M., Ucak, S., Kavruk, M., Ozalp, V.C., 2019. Anal. Biochem. 587, 113449.
Tomasi, C., Manduchi, R., 1998. Sixth International Conference on Computer Vision, pp. 839–846 (IEEE Cat. No.98CH36271).
Uyttendaele, M., Van Hoorde, I., Debevere, J., 2000. Int. J. Food Microbiol. 54 (3), 205–212.
Vygen-Bonnet, S., Rosner, B., Wilking, H., Fruth, A., Prager, R., Kossow, A., Lang, C., Simon, S., Seidel, J., Faber, M., Schielke, A., Michaelis, K., Holzer, A., Kamphausen, R., Kalhöfer, D., Thole, S., Mellmann, A., Flieger, A., Stark, K., 2017. Euro Surveill. 22 (21), 30541.
Wachi, K., Tateda, K., Yamashiro, Y., Takahashi, M., Matsumoto, T., Furuya, N., Ishii, Y., Akasaka, Y., Yamaguchi, K., Uchida, K., 2005. Intern. Med. 44 (12), 1316–1319.
Wang, Y., Salazar, J.K., 2016. Compr. Rev. Food Sci. Food Saf. 15 (1), 183–205.
Washburn, E.W., 1921. Phys. Rev. 17 (3), 273–283.
Wolffs, P.F.G., Glencross, K., Thibaudeau, R., Griffiths, M.W., 2006. Appl. Environ. Microbiol. 72 (6), 3896.
WorldHealthOrganization, 2019. Newsroom/fact sheets/detail/food safety. https://www.who.int/news-room/fact-sheets/detail/food-safety.
Yang, Y., Xu, F., Xu, H., Aguilar, Z.P., Niu, R., Yuan, Y., Sun, J., You, X., Lai, W., Xiong, Y., Wan, C., Wei, H., 2013. Food Microbiol. 34 (2), 418–424.
Zhao, F., Lee, E.Y., Noh, G.S., Shin, J., Liu, H., Qiao, Z., Shin, Y., 2019. Sci. Rep. 9 (1), 16374.
Zhou, B., Xiao, J., Liu, S., Yang, J., Wang, Y., Nie, F., Zhou, Q., Li, Y., Zhao, G., 2013. Food Control 32 (1), 198–204.